Theory of Tunneling Spectroscopy in a Mn_{12} Single-Electron Transistor by Density-Functional Theory Methods

Ł. Michalak,[1] C. M. Canali,[1] M. R. Pederson,[2] M. Paulsson,[1] and V. G. Benza[3]

[1]*Division of Physics, Department of Natural Sciences, Kalmar University, 391 82 Kalmar, Sweden*

[2]*Center for Computational Materials Science, Naval Research Lab, Code 6390, Washington, DC 20375, USA*

[3]*Dipartimento di Fisica e Matematica, Universita dell' Insubria, 20064 Como, Italy*

(Received 10 November 2008; revised manuscript received 2 November 2009; published 5 January 2010)

We consider tunneling transport through a Mn_{12} molecular magnet using spin density functional theory. A tractable methodology for constructing many-body wave functions from Kohn-Sham orbitals allows for the determination of spin-dependent matrix elements for use in transport calculations. The tunneling conductance at finite bias is characterized by peaks representing transitions between spin multiplets, separated by an energy on the order of the magnetic anisotropy. The energy splitting of the spin multiplets and the spatial part of their many-body wave functions, describing the orbital degrees of freedom of the excess charge, strongly affect the electronic transport, and can lead to negative differential conductance.

DOI: 10.1103/PhysRevLett.104.017202 PACS numbers: 75.50.Xx, 31.15.ej, 73.23.Hk, 85.65.+h

There is a growing interest in exploring the rich physics and spintronics functionality of molecular single-electron transistors (SETs) consisting of a few *magnetic* molecules weakly coupled to nanogapped electrodes [1]. Recently two groups [2,3] have carried out single-electron tunneling experiments on individual magnetic molecules based on $Mn_{12}O_{12}$ (henceforth Mn_{12}) with organic ligands. Mn_{12} is the most studied and perhaps the most remarkable molecular magnet [4]. In its crystal phase, Mn_{12} is characterized by a long spin relaxation time due to its large uniaxial magnetic-anisotropy energy. Furthermore, at low temperatures, quantum effects in the relaxation properties are clearly discernible [5–8] and have been attributed to quantum tunneling of the molecule collective magnetization [4]. How these properties are revealed in electronic quantum transport is a question of great significance for the field of molecular spintronics [1]. Indeed, the SET experiments [2,3] show signatures of the molecule magnetic state and its low-energy collective spin excitations. The theoretical models proposed so far [2,3,9–15] are typically based on effective giant-spin Hamiltonians with large uniaxial anisotropy barriers. This approach has two drawbacks [16]. First, the effective spin Hamiltonian for the charged states (anion and cation) of Mn_{12} needed to describe sequential tunneling transport, is not known. Scaling of the global anisotropy parameter to account empirically for changes in the number of electrons forming a macro-spin is fraught with uncertainty [17]. Second, the orbital degrees of freedom are not included in the giant-spin Hamiltonian formalism. The orbital effects due to changes in electron population on the Mn_{12} molecule modify the symmetry and magnitude of the magnetic-anisotropy Hamiltonian and can even change the spin ordering [18].

In this Letter we provide a microscopic many-body description of the ground state (GS) and low-lying spin excitations of both neutral and *charged* states of a Mn_{12} molecular magnet. Our approach is based on spin density functional theory (SDFT), which has been very successful in describing the spin-orbit-induced magnetic-anisotropy barrier in Mn_{12} and other molecular magnets [19–21]. We find that when a *delocalized* electron is added to (subtracted from) the molecule, the GS spin of the molecule increases (decreases) by $1/2$. For both charged states, the GS magnetic-anisotropy energy is larger than for the neutral Mn_{12}. We then incorporate this information into a quantum master equation for electronic transport in the sequential tunneling approximation, which is appropriate for the experimental Coulomb blockade (CB) regime. The approximate many-particle eigenstates lead to a tunneling conductance that exhibits fine structure on the order of the anisotropy energy and, under certain circumstances, to strong negative differential conductance (NDC). Comparison with the giant-spin model shows that spatial selection rules play a crucial role in determining which spin excitations contribute the most to the tunneling conductance.

We need to know the many-electron wave functions, representing low-energy spin excitations, as a function of the excess charge (Q), spin ordering ($\mathbf{M} \equiv \{\mu_\nu\}_{\nu=1,12}$), applied electric $\mathbf{E}$ and magnetic $\mathbf{B}$ fields, and the parameters θ, ϕ describing the quantization axes. We refer to the collection of all possible variables as the ''order-parameter vector'' (OPV), $\mathbf{p} \equiv (Q, \mathbf{M}, \mathbf{E}, \mathbf{B}, \theta, \phi)$ to label the states. Given a specific OPV, we first construct a set of Kohn-Sham (KS) single-particle states $\Phi_k(\mathbf{p})$, by diagonalizing a KS single-particle Hamiltonian $H(\mathbf{p})$ that depends upon this OPV. Since some of these effects (Q, $\mathbf{M}$) are clearly large and some (θ, ϕ) are generally small, there is flexibility as to which of these terms must be accounted for self-consistently. Specifically,

$$H(\mathbf{p}) = H(Q, \mathbf{M}, \mathbf{E}, \mathbf{B}, \theta, \phi) = H_0(\mathrm{DFT}, Q, \mathbf{M}) + V_{\mathbf{L}\cdot\mathbf{S}}(\theta, \phi) + \mathbf{E}\cdot\mathbf{r} + \mathbf{B}\cdot(\mathbf{L} + 2\mathbf{S}) \quad (1)$$

contains a spin-polarized term $H_0(\mathrm{DFT}, Q, \mathbf{M})$, which is treated self-consistently for the cation, neutral, and anionic states ($Q = +1, 0$ and -1); $V_{\mathbf{L}\cdot\mathbf{S}}(\theta, \phi)$ represents the spin-orbit interaction. We neglect the last two terms representing the coupling to external fields.

The spin-ordering $\mathbf{M}$ corresponds to that obtained from the local moments of the 12 Mn atoms (μ_ν) in the classical ferrimagnetic state of the neutral molecule [22]. The spin-orbit operator is treated exactly [19]—albeit non-self-consistently—in the basis of the eigenstates of $H_0(\mathrm{DFT}, Q, \mathbf{M})$. Diagonalizing the above Hamiltonian with the constraint that the expectation value of the total spin ($\langle\mathbf{S}\rangle$) is quantized along the axis determined by θ, ϕ results in a set of single-particle, *noncollinear* spin orbitals, $\phi_k(\mathbf{p})$, expressed as $\phi_k = \phi_k^+(r)\chi_+(\theta, \phi) + \phi_k^-(r)\chi_-(\theta, \phi)$. Here, the angle-dependent spinors $\chi_\pm(\theta, \phi)$ are spin-1/2 coherent states specified by the quantization axis, $\chi_\pm(\theta, \phi) = \cos(\theta/2)|\pm\rangle \pm \sin(\theta/2)e^{\pm i\phi}|\mp\rangle$.

We now construct approximate many-body functions for the ground and excited electronic states as single Slater determinants (SDs) of the spin orbitals $\phi_k(p)$:

$$|\mathbf{p}; k_1, k_2, \ldots, k_{N_Q}\rangle \equiv |\phi_{k_1}(\mathbf{p})\phi_{k_2}(\mathbf{p})\ldots\phi_{k_{N_Q}}(\mathbf{p})\rangle. \quad (2)$$

The above states are generally not eigenstates of either $\mathbf{S}^2$ or S_z. However, a state with $|\langle\mathbf{S}^2\rangle| = S_0(S_0 + 1)$, especially when constructed from a closed shell of spatial states, is expected to be the primary contributor to an $S = S_0$ eigenstate. While the variables (θ, ϕ) generate a continuous overdetermined set of SDs, a judicious choice of $2S_0 + 1$ values of θ and ϕ can lead to a nearly orthogonal set of normalized linearly independent many-particle SDs, with $\langle S_z\rangle$ taking on integer or half integer values akin to the standard $M = -S_0, -S_0 + 1, \ldots, S_0$ quantum numbers. Choosing $2S + 1$ values of θ given by $S\cos(\theta_M) = M$ leads to integer or half integer $\langle S_z\rangle$ regardless of the choice of ϕ; however, choosing $\phi_M = M\phi_0$ leads to destructive interference in the off-diagonal elements of these states and aids in producing approximate S_z eigenstates. For the case of $S = 10$, we find that choosing $\phi_0 = 34°$ leads to the smallest off-diagonal overlaps between approximate eigenstates. We call the $2S_0 + 1$ many-electron states constructed with this procedure a spin multiplet. Besides the GS spin multiplet, the anion and cation have a few low-lying excited spin multiplets. These come about because the HOMO level of the charged molecule is quasidegenerate with a many-fold of LUMO levels [18]. Using Eq. (2), we can construct several SD excited-states close in energy to the GS, all having the same spin, S_0. The relevant spin multiplets for the molecule are shown in Fig. 1(a). Typically, the level spacing within each spin multiplet is of the order of 0.1–1 meV, while different multiplets are separated by energies of the order of 10 meV. Note that the energies of a given spin multiplet are not exactly invariant under $M \to -M$, since the choice of the angle ϕ_M is incommensurate with the nonperfectly uniaxial symmetry of Mn_{12}. The breaking of the level degeneracy for the $(M, -M)$ pair is of the order of the transverse anisotropy terms coming from 4th order spin-orbit contributions, and therefore very small [23]. For a later comparison with the giant-spin approach, we disregard the small deviations from uniaxial symmetry and consider the spin Hamiltonian $H_{S_Q} = \sum_{i,n} D_{S_Q,i,n}[S^z_{Q,i}]^n$, given in terms of spin variables $\vec{S}_{Q,i}$ for each spin multiplet i of charge state Q; $D_{S_Q,i,n}$ are anisotropy constants which we extract by fitting the corresponding SDFT energy spectra. Table I shows the total spin, GS energy and magnetic-anisotropy energy of the lowest spin multiplet calculated for the different charge states of Mn_{12}. Adding an electron to the molecule increases the molecule spin and decreases the energy. Furthermore, the anisotropy increases significantly when a delocalized electron is added to the neutral molecule. This is due to the fact that there is a near degeneracy between unoccupied onefold and twofold states. The spin-orbit interaction leads to a strong mixing between these states which, because of the orbital components, enhances the anisotropy.

In the following we discuss quantum transport through a Mn_{12} molecule weakly coupled to metallic electrodes. Electron tunneling between leads and the molecule is described by the Hamiltonian $H_T = \sum_{\alpha,l}\sum_{k,\mathbf{p}} t_{\alpha l}a^\dagger_{\alpha l}c_k(\mathbf{p}) + \mathrm{H.c.}$, where $c_k^\dagger$ (c_k) creates (de-

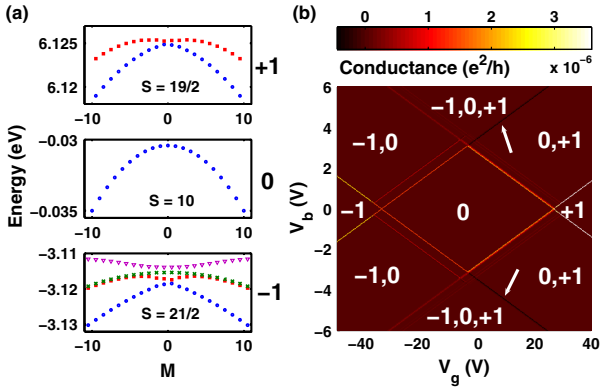

FIG. 1 (color online). (a) Lowest lying spin multiplets for the three charge states of the molecule; the small energy difference between states M and $-M$ is due to transverse anisotropy terms coming from 4th-order spin-orbit contributions and our choice of the $2S + 1$ values of (θ_M, ϕ_M). See text after Eq. (2). (b) Differential conductance of a Mn_{12} SET as a function of bias and gate voltage, for a symmetric double junction, with gate capacitance equal to 1/20 of the total capacitance, at zero temperature. Numbers -1, 0 and $+1$ denote the excess charge on the molecule and label regions of Coulomb blockade. In regions $(-1, 0)$, $(0, +1)$ and $(-1, 0, +1)$ transport is possible via transitions between different charge states.

TABLE I. The GS properties from DFT: spin, energy, and magnetic-anisotropy energy as a function of charge.

State	Q	Spin	Energy (eV)	MAE (K)	MAE (meV)
Anion	-1	21/2	-3.08	137	11.8
Neutral	0	20/2	0.00	55	4.7
Cation	1	19/2	6.16	69	5.9

stroys) an electron in orbital k in the molecule, and t_α depends on the tunneling barrier between lead $\alpha = L, R$ (left or right) and the molecule. The leads, at electrochemical potential μ_α, are described by the independent-electron Hamiltonian $H_\alpha = \sum_l \epsilon_{\alpha l} a^\dagger_{\alpha l} a_{\alpha l}$, where $a^\dagger_{\alpha l}$ ($a_{\alpha l}$) creates (destroys) a quasiparticle of quantum number l. We also take into account the work function for the external leads. As a result, the charge state populated at zero gate and bias voltages is the neutral one, and not the anion as it would seem from Table I. The sequential tunneling current is obtained from a master equation for the occupation probabilities of the molecule many-body states. The transition rate between two many-body states via tunneling of an electron from lead α into the molecule, is proportional to $f(E(\mathbf{p}', k'_i, N_{Q'}) - E(\mathbf{p}, k_i, N_Q) - \mu_\alpha) \times |\langle \mathbf{p}'; k'_1, k'_2, \ldots, k'_{N_{Q'}} | c^\dagger_k(\mathbf{p}) | \mathbf{p}; k_1, k_2, \ldots, k_{N_Q} \rangle|^2$, where $f(E)$ is the Fermi distribution function and $E(\mathbf{p}, k_i, N_Q)$ is the energy of state $|\mathbf{p}; k_1, k_2, \ldots, k_{N_Q}\rangle$, modified by the bias $V_b = (\mu_L - \mu_R)/e$ and gate voltage V_g. We then solve numerically the master equation in steady-state and obtain the current as a function of V_b and V_g. Figure 1(b) shows the differential conductance $G = dI/dV_b$ as function of V_b and V_g. The calculations are done at zero temperature. We choose equal coupling of the molecule to the two leads; the gate capacitance is equal to $1/20$ of the total capacitance of the system. Three CB stability diamonds are visible, corresponding to the three different charge states $Q = -1$, 0, $+1$, where transport is blocked. In region indicated by $(-1, 0)$, [respectively $(0, +1)$], current flows through transitions between anionic (cationic) and neutral states. In region $(-1, 0, +1)$ all three charge states are present. The additional lines parallel to the GS-GS transitions are due to transitions between excited states. In Fig. 1(b) we can also see two lines, indicated by arrows, that correspond to a decrease in the current with increasing V_b (NDC). These lines give the bias at which, for a given V_g, anionic states become occupied in the $(0, +1)$ region. NDC in Mn_{12}-SET has been observed experimentally [2].

For a better understanding of transport just above the CB gap, in Fig. 2(a) we plot the differential conductance as a function of V_b, for $V_g = -20$ V. Transport in this region is due to transitions between the spin multiplets of the neutral and anionic molecule. The conductance peak spectrum displays a rich fine structure, with peak spacing on the order of 0.1–1 meV, which corresponds to that seen in experiment [2,3]. The first set of peaks at the very onset of transport is caused by transitions between the GS spin multiplets. Surprisingly, the conductance in this region is very small, $G \leq 10^{-8} e^2/h$, as shown in the inset; it is practically invisible for transitions between the low-lying states (large $|M|$ and $|M'|$) and slightly larger for transitions between higher-lying states (small $|M|$ and $|M'|$). As we argue below, this is caused by the very small overlap of the *orbital* parts of the many-body wave functions of the two GS spin multiplets. The second set of peaks in Fig. 2(a), $V_b \geq 1.485$ V, corresponds to transitions between the GS spin multiplet of the neutral molecule and the first three excited spin multiplets of the anion. This cluster of resonances is largely determined by the first excited spin multiplet of the anion, since reaching this multiplet opens up transport also via other multiplets. In particular, the dominant peak seen in the figure is due to transitions between the lowest-energy states of the GS spin multiplet of the neutral molecule and the first excited spin multiplet of the anion, as shown in Fig. 2(b).

In order to shed light on the interplay between orbital and spin-selection rules, we compare the SDFT-based calculation with the giant-spin model. Within this spin model, transitions are possible only between states whose spin differs by 1/2 (spin-selection rule), with transition rates given by Clebsch-Gordan (CG) coefficients [24]. In the computation of the conductance, we include the GS spin multiplet of the neutral molecule, and the GS and first three excited spin multiplets of the anion. The conductance for the giant-spin model is shown with the dotted line in Fig. 2(a). The first 11 peaks correspond to subsequent transitions between states $M = \pm S, \pm(S-1), \ldots, 0$ and $M' = \pm S', \pm(S'-1), \ldots, 1/2$, where $S' = S + 1/2$. The intensity of these peaks decreases monotonically with decreasing $|M|$, which is different from the SDFT-

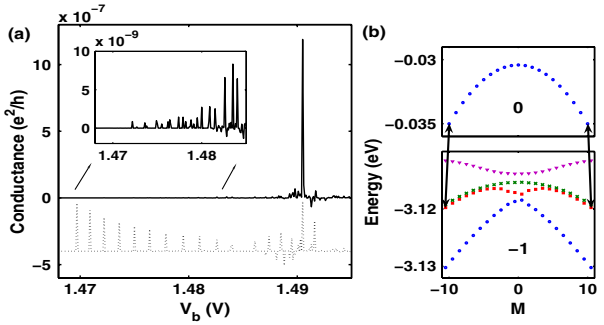

FIG. 2 (color online). (a) Differential conductance as a function of bias at $V_g = -20$ V. Parameters are as in Fig. 1. Solid (dotted, offset for clarity) lines: calculation based on SDFT (giant-spin model). Inset of (a) shows a zooming of the onset of SDFT transport due to transitions between the ground-state (GS) spin multiplets of the neutral and anionic molecule. Visible peaks in the main plot correspond to transitions between the GS spin multiplet of the neutral and the first three excited multiplets of the anion. (b) Spin multiplets involved in the transport. The transitions between the states generating the dominant peak in (a) are indicated by arrows joining the states.

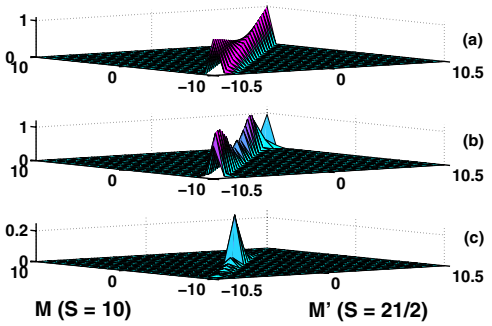

FIG. 3 (color online). Matrix elements for transitions between anionic and neutral charge states. (a) Giant-spin model; (b) SDFT results for transitions from neutral GS spin multiplet to anionic first excited multiplet; (c) SDFT results for transitions from neutral GS to anionic GS spin multiplets.

based conductance. The more complicated set of peaks at $V_b \geq 1.485$ V in Fig. 2(a) resembles the analogous cluster of peaks for SDFT and has the same interpretation. We examine the matrix elements giving the neutral-to-anion transition rates. Figure 3(a) shows the results for the giant-spin model, where the matrix elements are proportional to the CG coefficients and the spin-selection rule $|M - M'| = 1/2$ is strictly obeyed. Figure 3(b) shows that the same spin-selection rule is approximately satisfied by the SDFT matrix elements of the transitions between the GS spin multiplet of the neutral molecule and the first excited spin multiplet of the anion. In particular, the orbital part of the wave functions does not modify substantially this condition. In contrast, Fig. 3(c) shows that the SDFT matrix elements for the transition between the two GS spin multiplets are different: the effect of the spin-selection rules is now overridden by space selection rules, which suppress most of the transition rates near $|M| = S$ and lead to a vanishing conductance. Furthermore, the GS matrix elements close to the diagonal behave differently as a function of $|M|$ for the two models: they decrease with $|M|$ for SDFT and increase for the spin model, which is reflected in the conductance [Fig. 2(a)] for $V_b < 1.485$ V. Based on Figs. 3(a)–3(c), we expect the giant-spin model to agree better with the SDFT calculation for transitions involving the first excited-state spin multiplet of the anion. Indeed, Fig. 2(a) shows that for bias voltages $V_b \geq 1.485$ V the two models yield qualitatively the same conductance. The small matrix elements in Fig. 3(c) are also the cause of the NDC seen in Fig. 1(b) along the line separating the transport regions $(0, +1)$ and $(-1, 0, +1)$: when V_b becomes large enough to access the anion GS multiplet, the system remains trapped in these states due to their small connection to the neutral states. Thus, the current decreases.

In conclusion, we presented a microscopic study of the GS properties and low-energy spin excitations for the neutral and charged Mn_{12} molecular magnet, based on SDFT. Resonances in the tunneling conductance are governed both by spin and spatial selection rules. The latter ones play a key role in determining the relative contribution to transport of various spin multiplets, and can lead to NDC. The orbital properties of the spin states provided by SDFT are essential to build a correct effective spin model and interpret the transport experiments.

This work was supported by the Faculty of Natural Sciences at Kalmar University and the Swedish Research Council under Grant No. 621-2007-5019. M. R. P. thanks the DOD HPCMO for computational resources.

Note added.—After this manuscript was submitted, another Letter [25] related to our work appeared.

[1] L. Bogani and W. Wernsdorfer, Nature Mater. **7**, 179 (2008).
[2] H. B. Heersche *et al.*, Phys. Rev. Lett. **96**, 206801 (2006).
[3] M. H. Jo *et al.*, Nano Lett. **6**, 2014 (2006).
[4] D. Gatteschi, R. Sessoli, and J. Villain, *Molecular Nanomagnets* (Oxford, New York, 2006).
[5] R. Sessoli *et al.*, Nature (London) **365**, 141 (1993).
[6] L. Thomas *et al.*, Nature (London) **383**, 145 (1996).
[7] J. R. Friedman *et al.*, Phys. Rev. Lett. **76**, 3830 (1996).
[8] W. Wernsdorfer and R. Sessoli, Science **284**, 133 (1999).
[9] C. Romeike, M. R. Wegewijs, and H. Schoeller, Phys. Rev. Lett. **96**, 196805 (2006).
[10] C. Timm and F. Elste, Phys. Rev. B **73**, 235304 (2006).
[11] M. N. Leuenberger and E. R. Mucciolo, Phys. Rev. Lett. **97**, 126601 (2006).
[12] C. Timm, Phys. Rev. B **76**, 014421 (2007).
[13] F. Elste and C. Timm, Phys. Rev. B **75**, 195341 (2007).
[14] C. Romeike *et al.*, Phys. Rev. B **75**, 064404 (2007).
[15] G. Gonzalez, M. N. Leuenberger, and E. R. Mucciolo, Phys. Rev. B **78**, 054445 (2008).
[16] J. Lehmann and D. Loss, Phys. Rev. Lett. **98**, 117203 (2007).
[17] K. Park *et al.*, Phys. Rev. B **68**, 020405 (2003).
[18] K. Park and M. R. Pederson, Phys. Rev. B **70**, 054414 (2004).
[19] M. R. Pederson and S. N. Khanna, Phys. Rev. B **60**, 9566 (1999).
[20] M. Pederson *et al.*, Phys. Status Solidi B **217**, 197 (2000).
[21] J. Kortus *et al.*, Polyhedron **22**, 1871 (2003).
[22] J. Kortus, C. S. Hellberg, and M. R. Pederson, Phys. Rev. Lett. **86**, 3400 (2001).
[23] The breaking of the $M \rightarrow -M$ symmetry is the result of our approximation in constructing spin multiplets in terms of spin coherent states. Obviously *exact* eigenstates of a spin Hamiltonian would maintain the $M \rightarrow -M$ invariance, assured by time-reversal symmetry.
[24] C. M. Canali and A. H. MacDonald, Phys. Rev. Lett. **85**, 5623 (2000).
[25] S. Barraza-Lopez *et al.*, Phys. Rev. Lett. **102**, 246801 (2009).